

Report on -div A grad

Qile Yan

October 1, 2024

1 Problem setting

Let $A : \mathbb{R}^d \rightarrow \mathbb{R}^{d \times d}$ be a symmetric and uniformly elliptic field in the sense of

$$e \cdot A(x)e \geq \frac{1}{C_0}|e|^2, \quad |A(x)e| \leq |x|, \quad \text{for all } x, e \in \mathbb{R}^d.$$

In [1], they consider the acoustic operator

$$H_a := -\nabla \cdot A \nabla, \quad \text{on } L^2(\mathbb{R}^d).$$

where A is periodic, quasi-periodic or random.

What have been already done if the coefficient field A is random:

1. In Theorem 1.2 of [4], it was proved that when $d = 1$ and

$$A(x) = \frac{1}{1 + \sum_{n \in Z} f(x - n - d_n(\omega))}$$

where $\text{supp}(f) \subset [-s, s]$, $f \in L^1$, $1 + f > 0$, $f \neq 0$ and the displacements $\{d_n(\omega)\}$ are i.i.d random variables taking values in $[-d_{max}, d_{max}]$ with $d_{max} + s < 1/2$ then the operator H_a almost surely has dense pure point spectrum with exponentially decaying eigenfunctions.

2. In [5], they consider the case that the coefficient A is a random perturbation of a periodic function A_0 . They showed that the random operator H_a exhibits Anderson localization inside the gap in the spectrum of H_{a_0} .
3. In [1], the authors provides a strong control on the spatial spreading of the mass density of eigenstates in the lower spectrum. In particular, they proved a lower bound on the space width or localization length of an eigenstate ψ :

$$\ell_\theta(\psi) := \inf \left\{ r \geq 0 : \|\psi\|_{L^2(B_r)} \geq (1 - \theta) \|\psi\|_{L^2(\mathbb{R}^d)} \right\}, \quad 0 < \theta < 1/2.$$

With some assumptions on the random field, they showed that given $0 < \theta < 1/2$ and $\varepsilon > 0$, there exists a positive random variable $\lambda_{\theta, \varepsilon}$ such that: if H_a has an eigenvalue $\lambda \leq \lambda_{\theta, \varepsilon}$, any associated eigenstate ψ_λ satisfies

$$\ell_\theta(\psi_\lambda) \geq \begin{cases} \lambda^{\varepsilon - \frac{2}{3}} & : d = 1 \\ \lambda^{\varepsilon - \frac{1}{2}(\lfloor \frac{d}{2} \rfloor + 1)} & : d > 1 \end{cases}.$$

Some open problems raised from those forwarded emails :

1. Can one prove that there is always an interval of delocalization in 2D?
2. Is 3D indeed more delocalizing?

Some discussions: Recall that for the operator $L = -\Delta + V$, one can define its landscape function u as the solution to $Lu = 1$. The conjugation of L is defined as

$$\tilde{L}g = -\frac{1}{u^2}\operatorname{div}(u^2\nabla g) + \frac{1}{u}g.$$

Then $L\psi = \lambda\psi$ if and only if $\phi := \psi/u$ satisfies $\tilde{L}\phi = \lambda\phi$.

Now, the eigenvalue problem is

$$-\operatorname{div}(A\nabla u) = \lambda u.$$

We may check the eigenfunctions of the following operator

$$-\operatorname{div}(A\nabla u) = \lambda Au.$$

In the numerical experiment, we also test the following

$$-\operatorname{div}(\nabla u) = \lambda Au$$

2 Numerical experiment

One simple way to describe the localization of eigenfunction is the participation ratio of an eigenfunction which is defined as

$$\operatorname{PR}(f) = \frac{1}{|\Omega|} \frac{\left(\int_{\Omega} |f|^2\right)^2}{\int_{\Omega} f^4}.$$

Note that $0 \leq \operatorname{PR}(f) \leq 1$.

2.1 1d random displacement model in [4]

In Theorem 1.2 of [4], it was proved that when $d = 1$ and

$$A(x) = \frac{1}{1 + \sum_{n \in \mathbb{Z}} f(x - n - d_n(\omega))}$$

where $\operatorname{supp}(f) \subset [-s, s]$, $f \in L^1$, $1 + f > 0$, $f \neq 0$ and the displacements $\{d_n(\omega)\}$ are i.i.d random variables taking values in $[-d_{max}, d_{max}]$ with $d_{max} + s < 1/2$ then the operator H_a almost surely has dense pure point spectrum with exponentially decaying eigenfunctions.

The test codes is under the folder:grad_A_div/1d

Consider solving

$$-(Au)' = \lambda u$$

on a closed interval $[x_0, x_1]$. Let $s = 1/4$ and define

$$f(x) = 1/8[\max\{(1-x^2/s^2)^3, 0\}(3x^2+1)]' = \begin{cases} \frac{6}{8}x(1-x^2/s^2)^3 - \frac{6}{8s^2}x(1-x^2/s^2)^2(3x^2+1) & x \in [-s, s] \\ 0, & x \notin [-s, s] \end{cases}$$

Then $\text{supp}(f) \subset [-s, s]$, $f \in C^1$, $1 + f > 0$. See Fig.1 for the f .

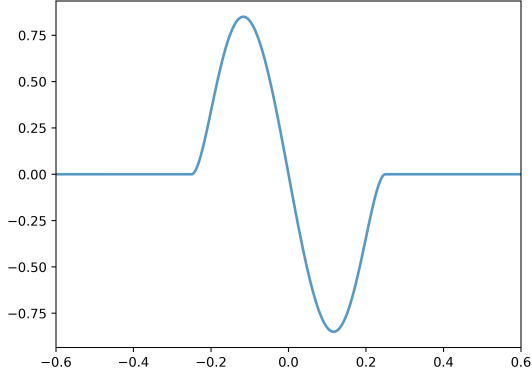


Figure 1: function f . code in grad_A_div/1d/test.py.

Let

$$A(x) = \frac{1}{1 + \sum_{n \in Z, x_0+1 \leq n \leq x_1-1} f(x - n - d_n(\omega))}$$

where the displacements $\{d_n(\omega)\}$ are i.i.d random variables taking values in $[-d_{max}, d_{max}]$ with $d_{max} = 1/5$.

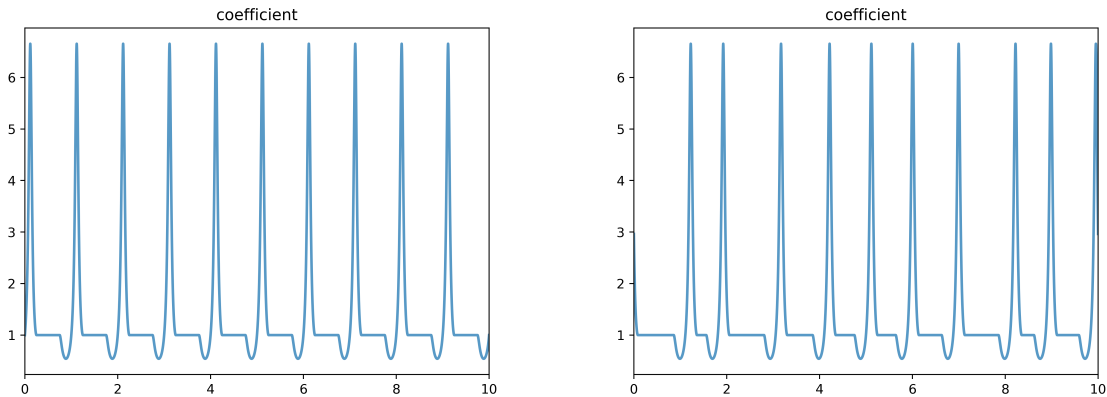


Figure 2: Coefficients on $[0, 10]$. (a). $d_{max} = 0$, i.e., no randomness and 1-periodic. (b) $d_{max} = 0.2$.

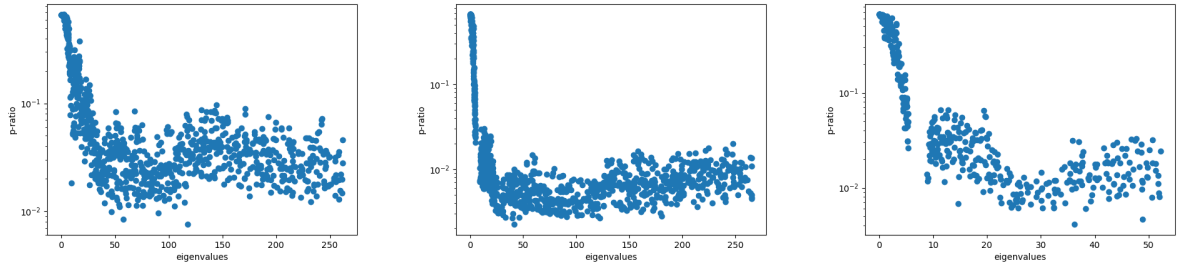


Figure 3: Over $[0, 200]$, Dirichlet boundary, $d_{max} = 0.2$. Participation ratio of first 500 eigenvalues.
 (a). $-\operatorname{div}(A\nabla u) = \lambda u$. (Results in 1d/Results/000015) (b). $-\operatorname{div}(A\nabla u) = \lambda Au$. (Results in 1d/Results/000016) (c). $-\operatorname{div}(\nabla u) = \lambda Au$. (Results in 1d/Results/000017)

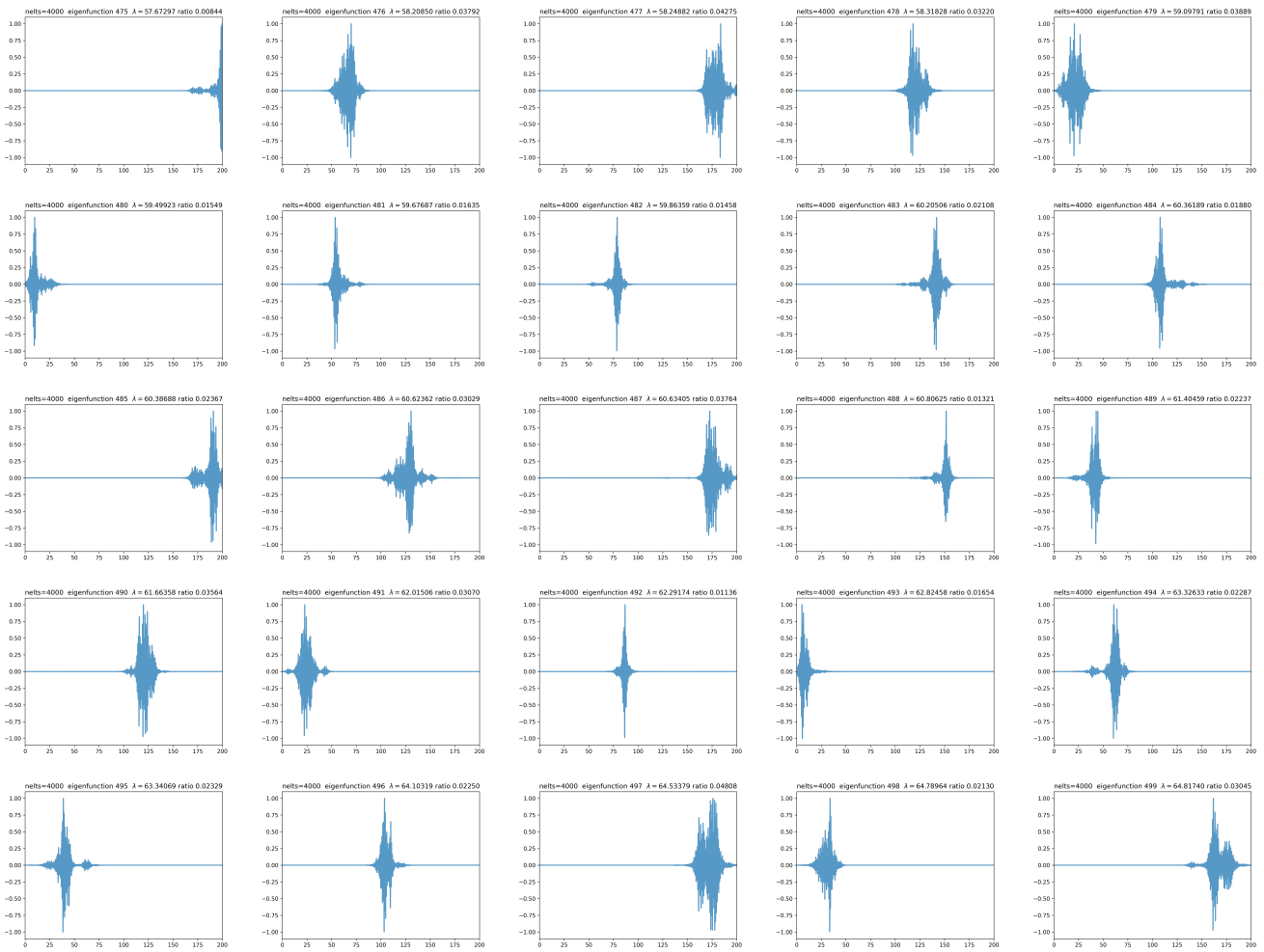


Figure 4: Over $[0, 200]$, Dirichlet, $d_{max} = 0.2$. modes 475 to 499. $-\operatorname{div}(A\nabla u) = \lambda u$. (Results in 1d/Results/000015)



Figure 5: Over $[0, 200]$, Dirichlet, $d_{max} = 0.2$. modes 475 to 499. $-\operatorname{div}(A \nabla u) = \lambda A u$. (Results in 1d/Results/000016)

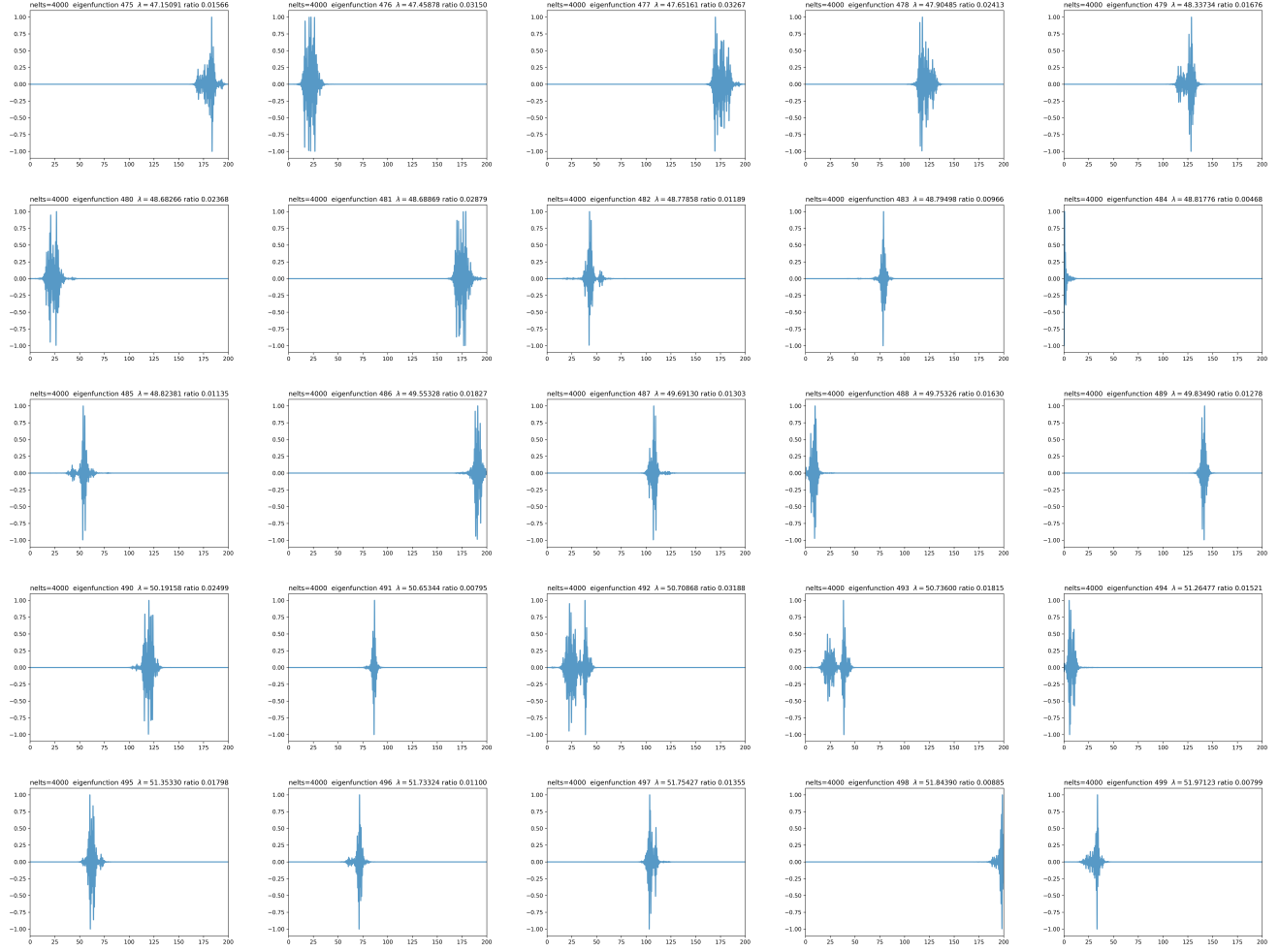


Figure 6: Over $[0, 200]$, Dirichlet, $d_{max} = 0.2$. modes 475 to 499. $-\operatorname{div}(\nabla u) = \lambda Au$. (Results in 1d/Results/000017)

2.2 2d random displacement model

Consider solving

$$-\operatorname{div}(A\nabla u) = \lambda u$$

on a closed square $[0, L] \times [0, L]$. Here,

$$A(x) = \frac{1}{1 + \sum_{n_1, n_2 \in \mathbb{Z}} f(x - (n_1, n_2) - d_n(\omega))}$$

where $\operatorname{supp}(f) \subset B_s(0)$, $f \in L^1$, $1 + f > 0$, $f \neq 0$ and the displacements $\{d_n(\omega)\}$ are i.i.d random variables taking values in $B_{d_{max}}(0)$ with $d_{max} + s < 1/2$. Let $s = 1/4$ and define

$$f(x) = 20 \max\{(1 - |x|^2/s^2)^3, 0\} (3|x|^2 + 1) = \begin{cases} 20(1 - |x|^2/s^2)^3(3|x|^2 + 1), & x \in B_s(0) \\ 0, & x \notin B_s(0) \end{cases}$$

Then $\operatorname{supp}(f) \subset B_s(0)$, $1 + f > 0$.

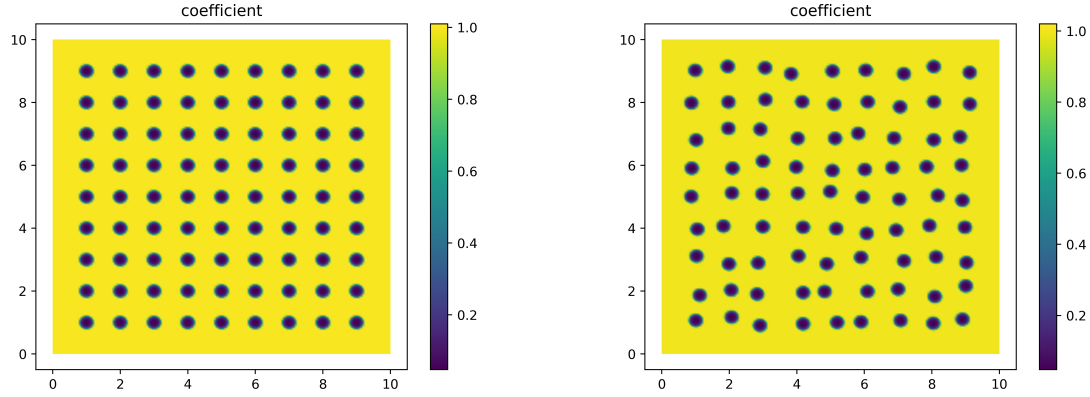


Figure 7: Coefficients on $[0, 10] \times [0, 10]$. (a). $d_{max} = 0$, i.e., no randomness. (b) $d_{max} = 0.2$.

Results over $[0, 100] \times [0, 100]$ are put in the following folders:

1. $-\operatorname{div}(A\nabla u) = \lambda u$. 2d/Results/000003
2. $-\operatorname{div}(A\nabla u) = \lambda Au$. 2d/Results/000004
3. $-\operatorname{div}(\nabla u) = \lambda Au$. 2d/Results/000005

So far, no localized eigenfunctions are found.

3 2d piecewise constant

Let $A(x)$ be a piecewise constant function with randomly chosen i.i.d. values from $[1, 10]$.

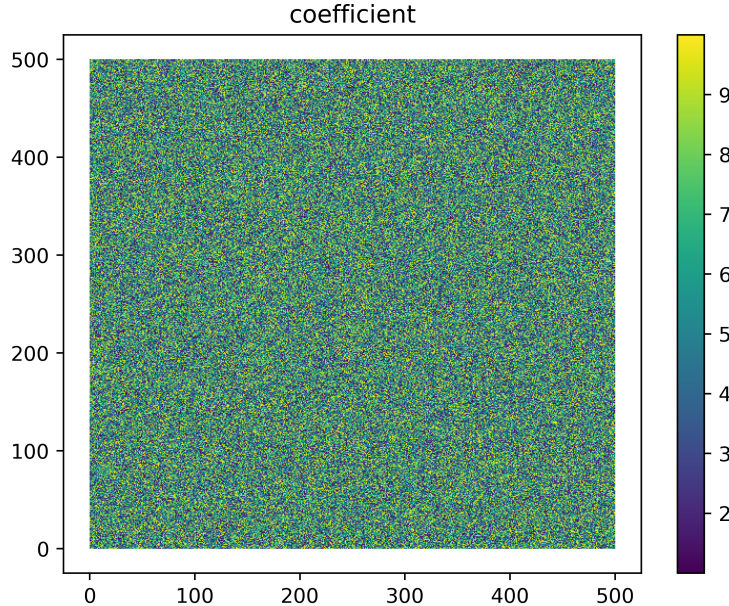


Figure 8: Coefficients on $[0, 500] \times [0, 500]$.

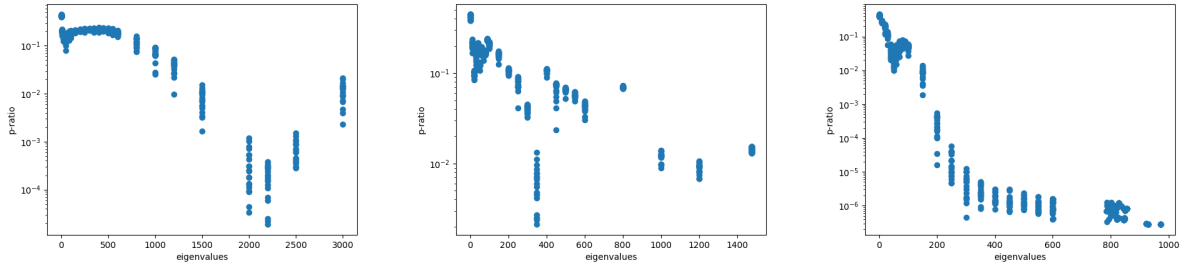


Figure 9: Over $[0, 500] \times [0, 500]$, Dirichlet boundary. Participation ratio vs eigenvalues. (a). $-\operatorname{div}(A\nabla u) = \lambda u$. (Results in 2d/Results/000014/pratio_eigen_log.png) (b). $-\operatorname{div}(A\nabla u) = \lambda Au$. (Results in 2d/Results/000015/pratio_eigen_log.png) (c). $-\operatorname{div}(\nabla u) = \lambda Au$. (Results in 2d/Results/000016/pratio_eigen_log.png). For each case, find the first 21 eigenvalues which are closest to the targets numbers: 0, 10, 20, 30, 40, 50, 60, 70, 80, 90, 100, 150, 200, 250, 300, 350, 400, 450, 500, 550, 600, 800, 1000, 1200, 1500, 2000, 2200, 2500, 3000.

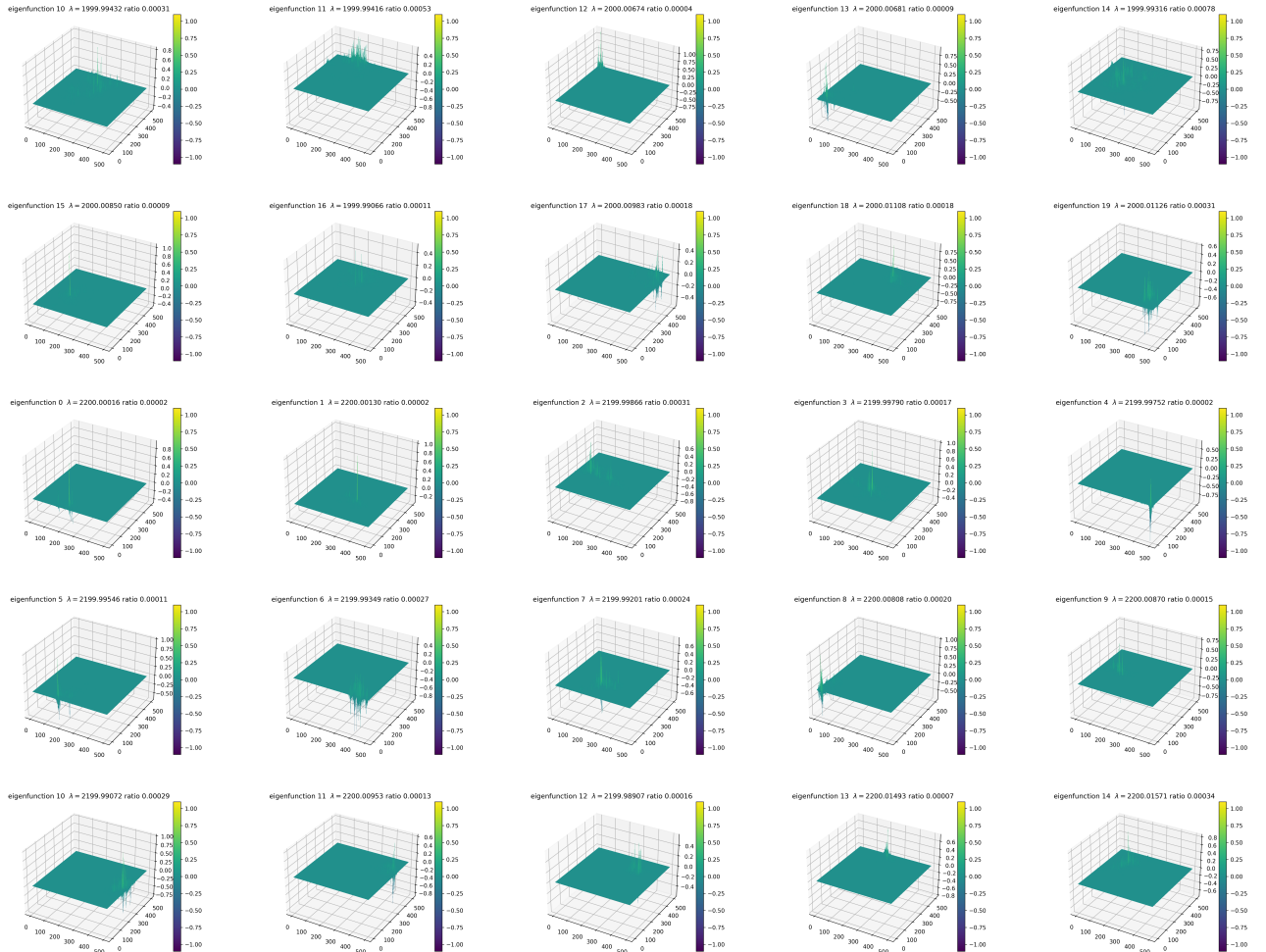


Figure 10: Over $[0, 500] \times [0, 500]$, Dirichlet. $-\operatorname{div}(A\nabla u) = \lambda u$. (Results in 2d/Results/000014/eigenfunmontage_smpr_00050.png)

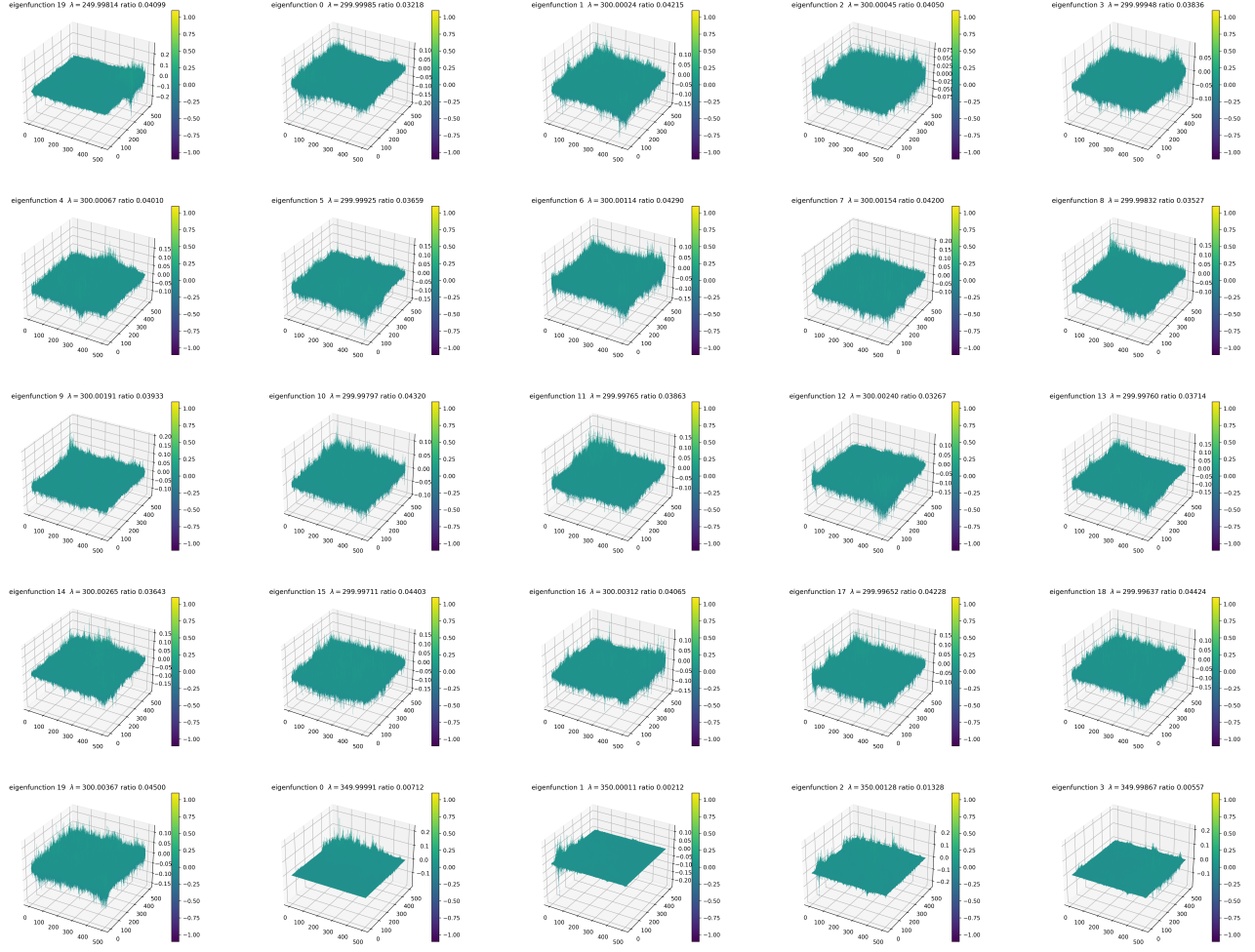


Figure 11: Over $[0, 500] \times [0, 500]$, Dirichlet. $-\operatorname{div}(A \nabla u) = \lambda Au$. (Results in 2d/Results/000015/eigenfunmontage_smpr_00000.png)

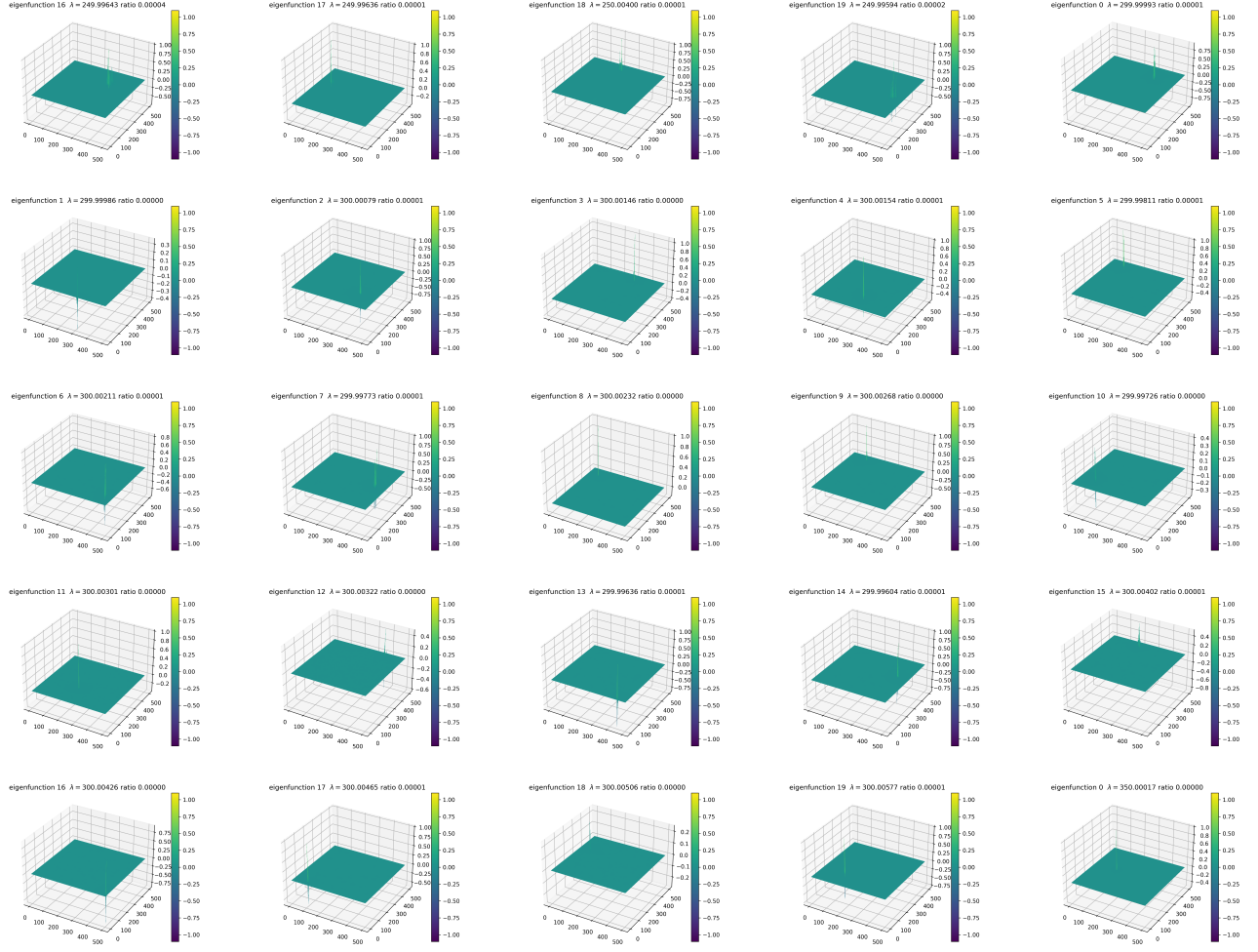


Figure 12: Over $[0, 500] \times [0, 500]$, Dirichlet. $-\operatorname{div}(\nabla u) = \lambda Au$. (Results in 2d/Results/000016/eigenfunmontage_smpr_00125.png)

4 Some 1D results on $-\operatorname{div}(A\nabla\phi) = A\lambda\phi$

Check for different size of interval L .

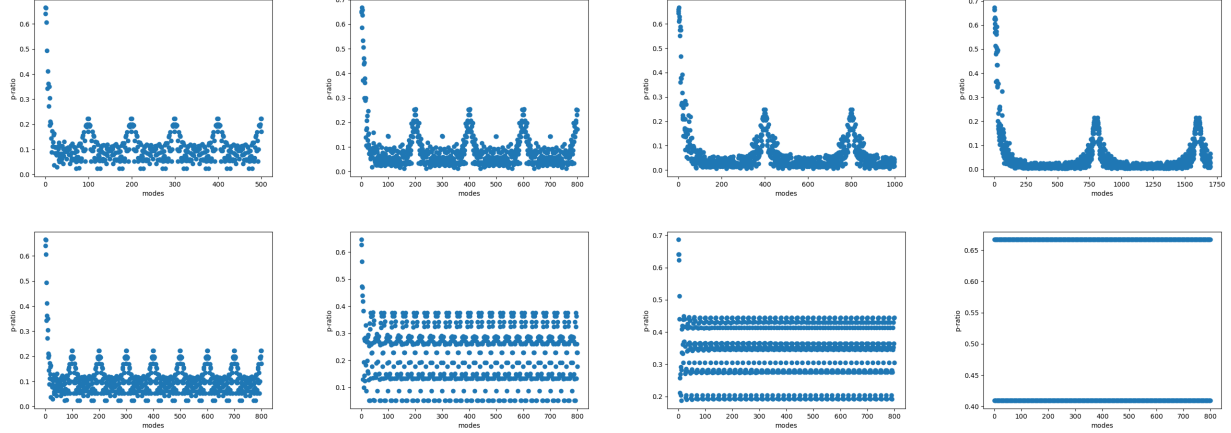


Figure 13: Participation ratio vs modes. pc coefficients with i.i.d from $[1,10]$, $-\operatorname{div}(A\nabla\phi) = A\lambda\phi$, Dirichlet boundary. **First row:** piecewise constant defined over interval with size 1. (a). $L = 100$. (Results/000029) (b). $L = 200$. (Results/000028) (c). $L = 400$. (Results/000019) (d). $L = 800$. (Results/000030) **Second row:** $L = 200$. nc : number of piecewise constants. (e). $nc = 100$. (Results/000031)(f). $nc = 40$. (Results/000032)(g). $nc = 20$. (Results/000033) (h). $nc = 2$. (Results/000034) Observation: the participation ratio is periodic in nc .

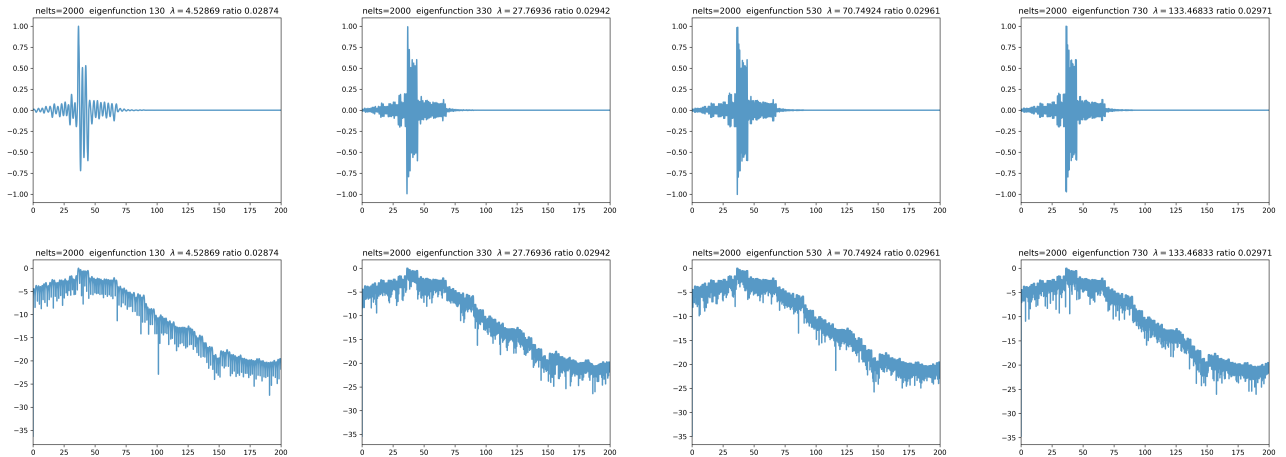


Figure 14: pc coefficients with i.i.d from $[1,10]$, $-\operatorname{div}(A\nabla\phi) = A\lambda\phi$, Dirichlet boundary. $L = 200$. First row: plot of eigenfunctions ψ . (Results/000028) Second row: plot of $\log(|\psi|)$. (Results/000028_logplot)

Check for different range of pc coefficients A .

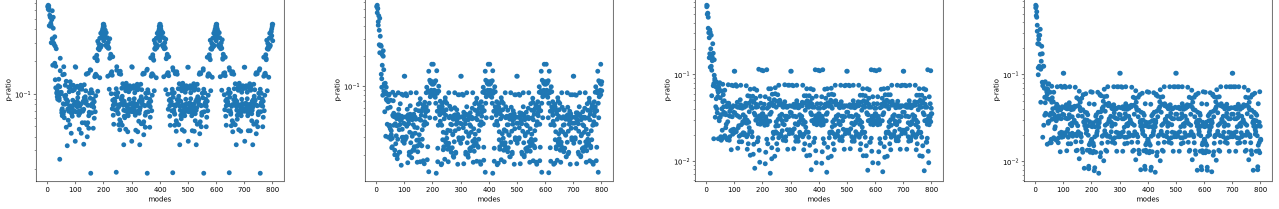


Figure 15: pc coefficients with i.i.d from $[1, V]$, $-\operatorname{div}(A \nabla \phi) = A \lambda \phi$, Dirichlet boundary. $L = 200$.
(a). $V = 5$. (Results/000036) (b). $V = 20$. (Results/000037) (c). $V = 50$. (Results/000038) (d).
 $V = 100$. (Results/000039) The plot of $V = 100$ is almost the same as the case $V = 200$.

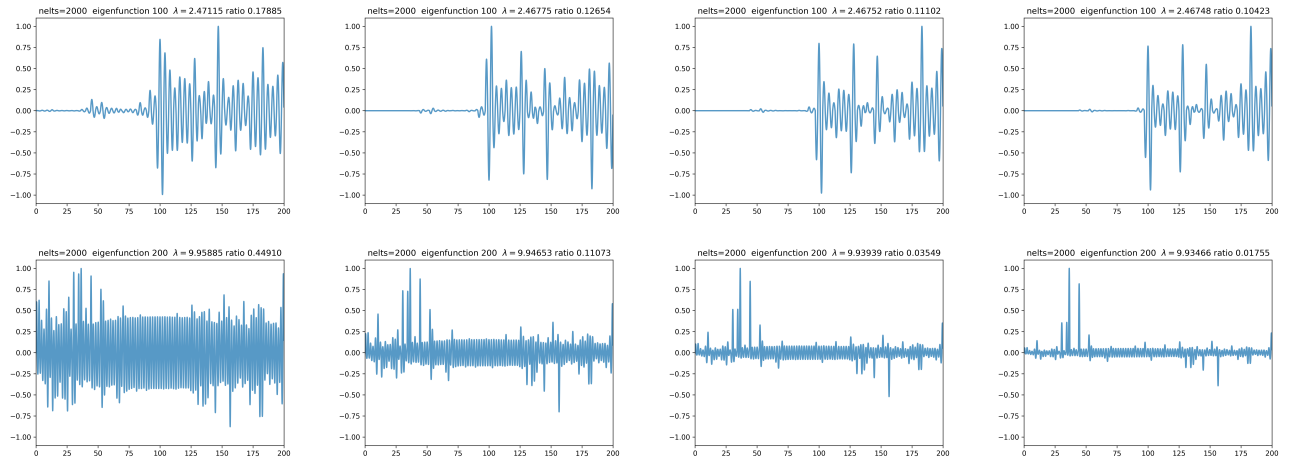


Figure 16: pc coefficients with i.i.d from $[1, V]$, $-\operatorname{div}(A \nabla \phi) = A \lambda \phi$, Dirichlet boundary. $L = 200$. First column: $V = 5$. Second column $V = 20$. Third column $V = 50$. Fourth column: $V = 100$.

Check $-\operatorname{div}(u^2 \nabla \phi) = \lambda u^2 \phi$ where u is the landscape function

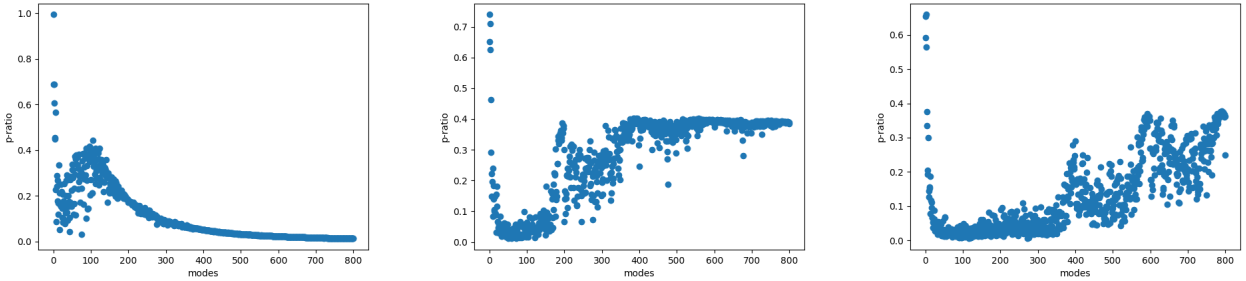


Figure 17: $-\operatorname{div}(u^2 \nabla \phi) = \lambda u^2 \phi$ where u is the landscape function with piecewise potential function i.i.d from $[0, V]$. Dirichlet boundary. $L = 200$. (a). $V = 1$. (Results/000054) (b). $V = 20$. (Results/000057) (c). $V = 100$. (Results/000053)

5 Some 2D results on $-\operatorname{div}(A\nabla\phi) = A\lambda\phi$

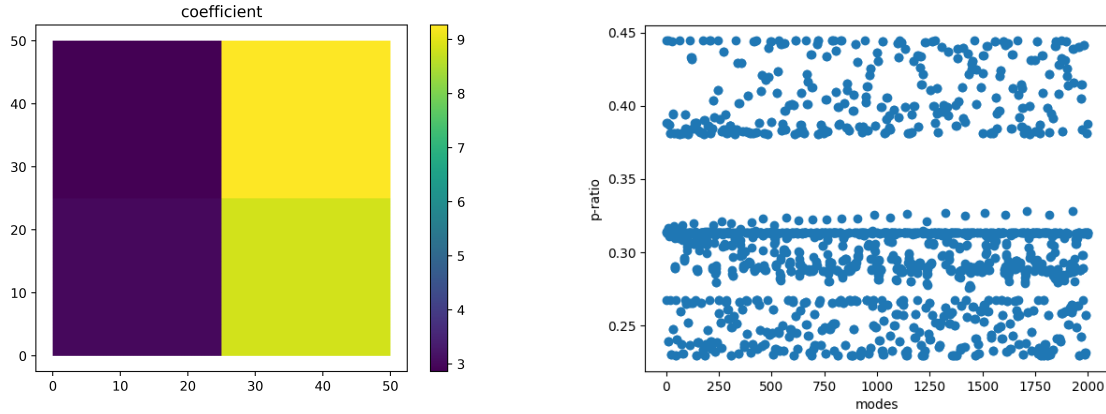


Figure 18: Over $[0, 50] \times [0, 50]$. pc coefficients with i.i.d from $[1,10]$, $-\operatorname{div}(A\nabla\phi) = A\lambda\phi$, Dirichlet boundary. $nc = 4$. (2d/Results/000017) (a) coefficients. (b). participation ratio vs modes

6 Numerical Tests

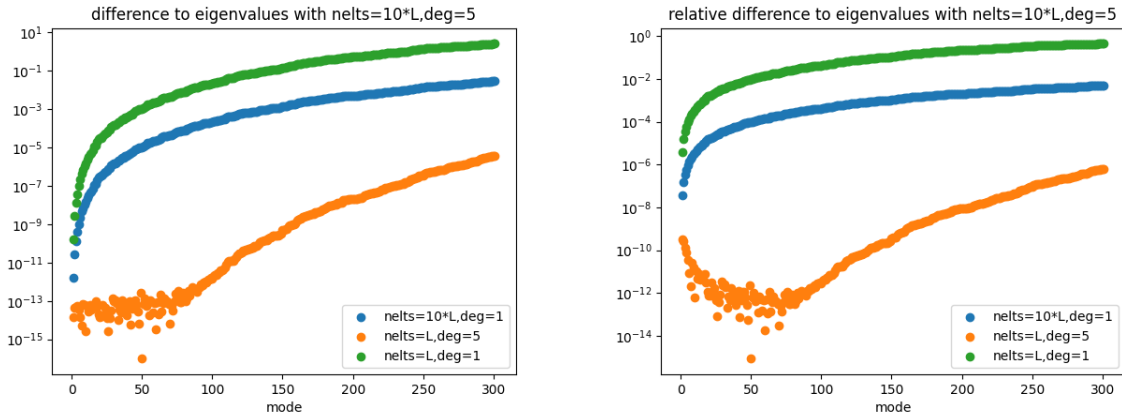


Figure 19: Over $[0, 400]$. pc coefficients with i.i.d from $[1,10]$, $-\operatorname{div}(A\nabla\phi) = A\lambda\phi$, Dirichlet boundary all first 300 eigenvalue. It seems that it is enough to take unit interval as one element with high degree polynomial.

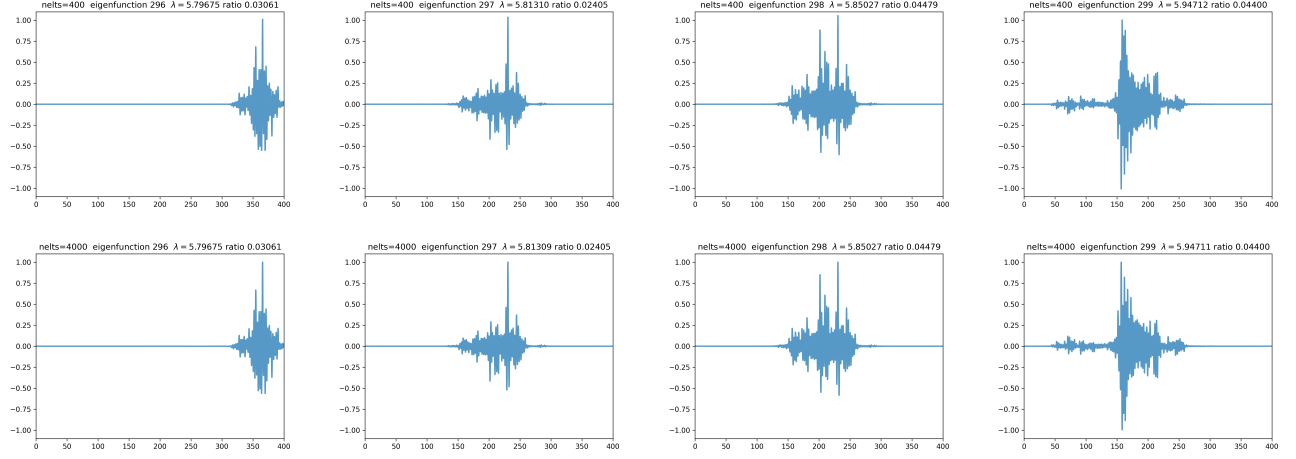


Figure 20: Over $[0, 400]$. pc coefficients with i.i.d from $[1,10]$, $-\operatorname{div}(A \nabla u) = A \lambda u$, Dirichlet boundary all first 300 eigenvalue. First row: $\text{nelts} = L$, $\text{deg} = 5$. (Results/000023) Second row: $\text{nelts} = 10L$, $\text{deg} = 5$. (Results/000021)

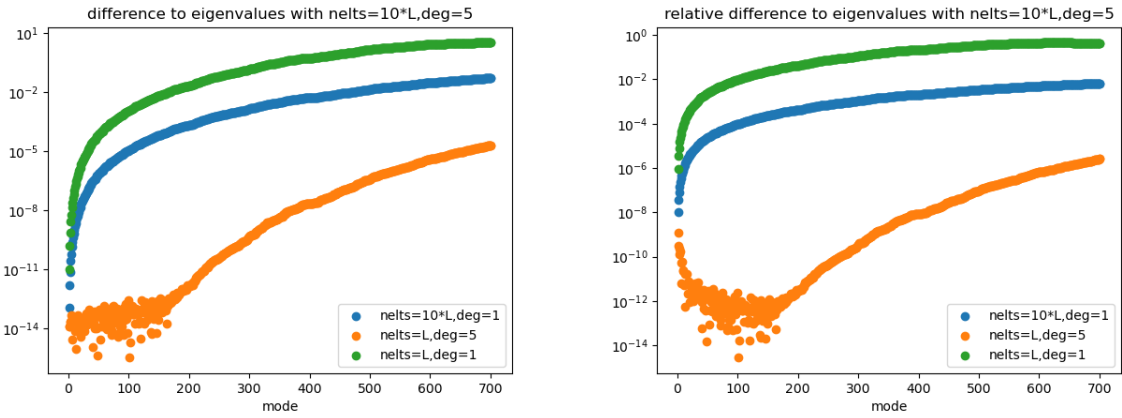


Figure 21: Over $[0, 800]$. pc coefficients with i.i.d from $[1,10]$, $-\operatorname{div}(A \nabla \phi) = A \lambda \phi$, Dirichlet boundary all first 300 eigenvalue. It seems that it is enough to take unit interval as one element with high degree polynomial.

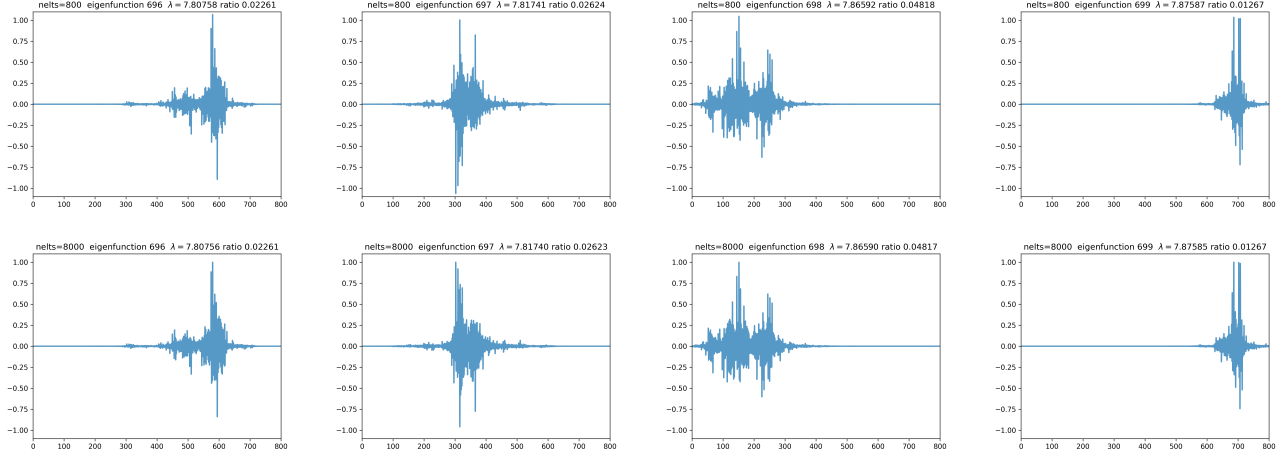


Figure 22: Over $[0, 800]$. pc coefficients with i.i.d from $[1,10]$, $-\operatorname{div}(A\nabla u) = A\lambda u$, Dirichlet boundary all first 300 eigenvalue. First row: $\text{nelts}=\text{L}$. $\text{deg}=5$. (Results/000027) Second row: $\text{nelts}=10\text{L}$, $\text{deg}=5$. (Results/000025)

7 Comparison with the Chapter 4 of the thesis [9]

Recall that for the operator $L = -\Delta + V$, one can define its landscape function u as the solution to $Lu = 1$. The conjugation of L is defined as

$$\tilde{L}g = -\frac{1}{u^2}\operatorname{div}(u^2\nabla g) + Wg.$$

where $W = \frac{1}{u}$ the effective confining potential.

To study the high-energy localization of \tilde{L} , Chapter 4 of [9] investigates the properties of the reduced equation:

$$-\frac{1}{u^2}\operatorname{div}(u^2\nabla\phi) = E\phi.$$

since at high energies the potential term can be neglected.

Numerically, they used following quantity to investigate the localization:

- (1) The participation ratio

$$\text{PR}_n = \frac{\left(\int |\psi_n|^2 dx\right)^2}{|\Omega| \int |\psi_n|^4 dx}.$$

- (2) Distribution of the energy spacings. Compute all the eigenvalues in a certain interval, then calculate the difference of the subsequent eigenvalues

$$s_n = E_n - E_{n-1}.$$

the energy spacings. Then divide these spacings by their average $\delta = \langle s \rangle$ to normalize the distribution. Two types of distributions:

- (i) The Poisson distribution: $P_P(s) = \frac{1}{\delta} \exp\left(-\frac{s}{\delta}\right)$ which corresponds to localized eigenfunctions. For a random matrix with zero off-diagonal elements, there is a completely random sequence of eigenvalues and the spacing has a Poisson distribution [10].

- (ii) The Wigner surmise distribution $P_{\text{GOE}}(s) = \frac{\pi}{2} s \exp\left(-\frac{\pi}{4}s^2\right)$, which linked to delocalized eigenfunctions. Here GOE means Gaussian Orthogonal Ensemble matrices (symmetric matrix with the upper triangular entries have distribution $N(0, 1)$ and the diagonal entries have distribution $N(0, 2)$). It was proved by M.L. Mehta in 1960 that the spacings of GOE follows a probability which is very close to the Wigner distribution.

The coefficient of determination R^2 will be calculated. It is difficult to determine when considering a very large range of eigenvalues.

- (3) The energy spacings ratios:

$$r_n = \min(s_n, s_{n+1}) / \max(s_n, s_{n+1})$$

For localized eigenfunctions, the distribution is $P_l(r) = 2/(1+r)^2$ with support $[0, 1]$ and its average is $\langle r \rangle_P = 2 \ln 2 - 1 \approx 0.386$. For delocalized eigenstates, the distribution is not known analytically. The numerical value for the average of the ratios: $\langle r \rangle \approx 0.5295$.

1D case: low-energy eigenfunctions are localized and their localization lengths increase with energy.

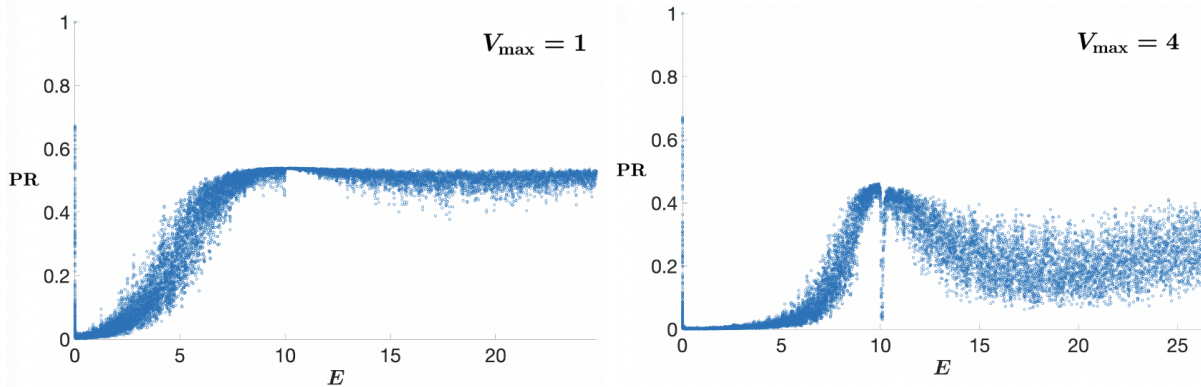


Figure 23: Fig 4.3 in [9]. The domain size is 10,000. The PR of all eigenfunctions of the reduced equation from $E = 0$ to $E = 25$. (a). $V_{\max} = 1$. (b). $V_{\max} = 4$.

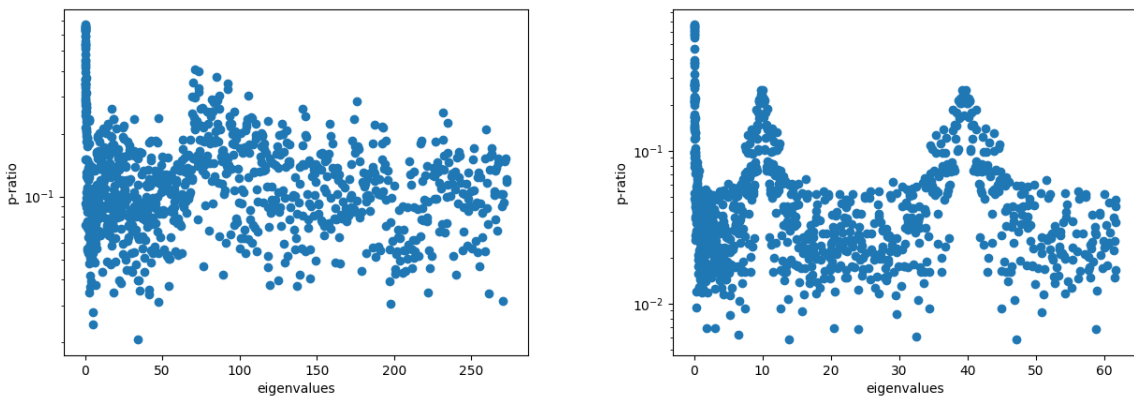


Figure 24: Over $[0, 400]$. Piecewise constant i.i.d from $[1, 10]$. (a) $-\text{div}(A\nabla\phi) = \lambda\phi$, (b) $-\text{div}(A\nabla\phi) = A\lambda\phi$

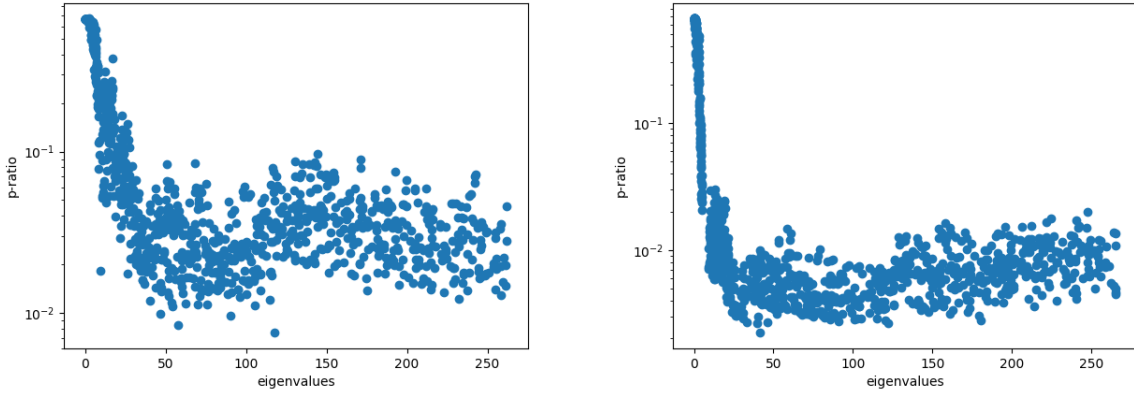


Figure 25: Over[0,200]. random displacement. (a) $-\operatorname{div}(A \nabla \phi) = \lambda \phi$, (b) $-\operatorname{div}(A \nabla \phi) = A \lambda \phi$

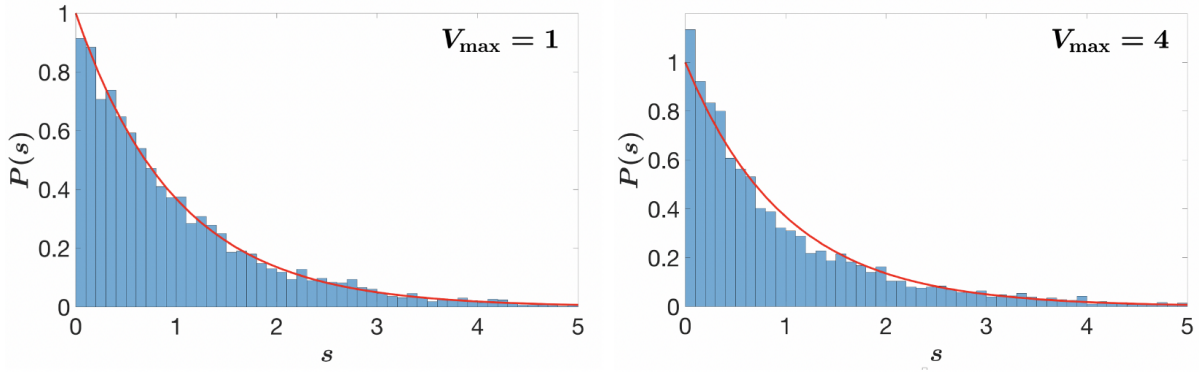


Figure 26: Fig 4.7 in [9]. Energy spacings. The domain size is 10,000. about 10,000 eigenfunctions starting at the beginning. The 1000 first eigenvalues of the reduced equations are excluded since the first eigenfunctions are always delocalized. The exact Poisson distribution in red. (a). $V_{max} = 1$. (b). $V_{max} = 4$.

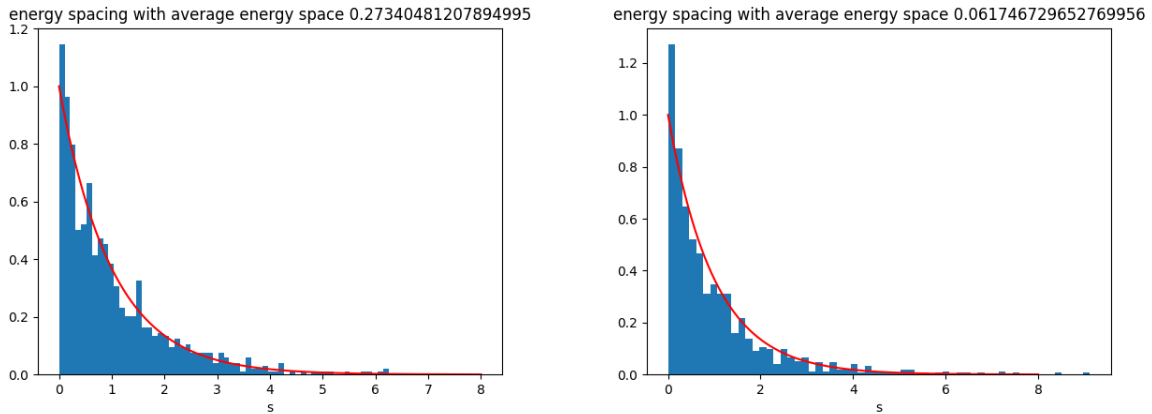


Figure 27: Energy spacings. Over[0,400]. $A(x)$ is piecewise constant i.i.d from [1, 10]. 1000 eigenfunctions (a) $-\operatorname{div}(A \nabla \phi) = \lambda \phi$, (b) $-\operatorname{div}(A \nabla \phi) = A \lambda \phi$

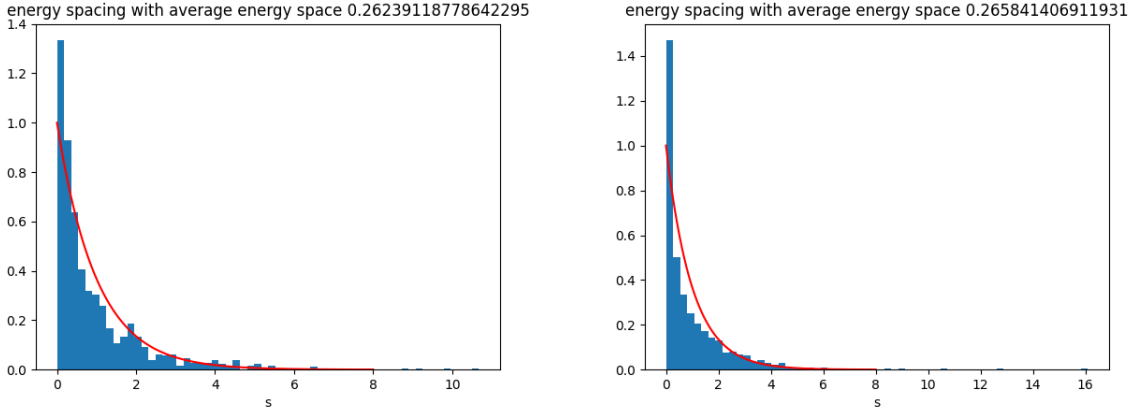


Figure 28: Energy spacings. Over $[0, 200]$. $A(x)$ is random displacement. 1000 eigenfunctions (a) $-\operatorname{div}(A\nabla\phi) = \lambda\phi$, (b) $-\operatorname{div}(A\nabla\phi) = A\lambda\phi$

2D: No localization delocalization transition, all the eigenfunctions remain localized.

References

- [1] DUERINCKX, MITIA and GLORIA, ANTOINE. Large-scale dispersive estimates for acoustic operators: homogenization meets localization. *Preprint* (2023)
- [2] Bordenave, Charles, Arnab Sen, and Balint Virág. Mean quantum percolation. *Journal of the European Mathematical Society* 19.12 (2017): 3679-3707.
- [3] Kuchment, Peter. An overview of periodic elliptic operators. *Bulletin of the American Mathematical Society* 53.3 (2016): 343-414.
- [4] Sims, Robert, and GÃ©Enter Stolz. Localization in One Dimensional Random Media: A Scattering Theoretic Approach *Communications in Mathematical Physics* 213 (2000): 575-597.
- [5] Figotin, Alexander, and Abel Klein Localization of classical waves I: Acoustic waves. *Communications in Mathematical Physics* 180.2 (1996): 439-482.
- [6] Kuchment, Peter An overview of periodic elliptic operators *Bulletin of the American Mathematical Society* no.3 (2016): 343-414.
- [7] Filonov, N Second-order elliptic equation of divergence form having a compactly supported solution *Journal of Mathematical Sciences* 106 (2001): 3078–3086.
- [8] Armstrong, Scott and Kuusi, Tuomo and Smart, Charles Large-Scale Analyticity and Unique Continuation for Periodic Elliptic Equations *Communications on Pure and Applied Mathematics* 76 (2023): 73–113
- [9] Desforges, Perceval Analysis of the spatial and spectral structures of localized eigenfunctions in Anderson models through the localization landscape theory *Diss. Institut Polytechnique de Paris* (2021)

- [10] Shklovskii, BI and Shapiro, B and Sears, BR and Lambrianides, P and Shore, HB Statistics of spectra of disordered systems near the metal-insulator transition *Physical Review B* 47 (1993): 11487